Chapter 4

Characterization of Haul Road Dust and Synthesized Polymers

4.1 Introduction

Main objective of the thesis work is to study the efficacy of the laboratory synthesized water-soluble polymers as suppressant for coal mine haul road dust. Therefore, it is important to have a detailed discussion about the characteristics of both these materials – haul road dust and the developed polymers.

4.2 Characterization of Haul Road Dust

The size distribution of haul road dust was carried out by sieve analysis. Elemental composition of dust was identified by energy dispersive X-ray (EDX) spectroscopy.

4.2.1 Size distribution

In the present study, a haul road dust sample was screened by sieves ranging from 2 mm to 74 μm size (Table 4.1). Silt is the fraction of haul road dust having particle size below 74 μm i.e. particles passing through 200 mesh size [100]. In the study, silt content was found to

be 20% of the total dust weight percentage. The significance of the silt content is that the probability of dust emission from haul road is increased as the percentage of silt content increases [101].

Table 4.1 Particle size distribution (%) of dust sample

mesh size	mm	Wt. of Particle	% Wt.	Cumulative %	% Finer by Mass
10	2	0	0	0	100
12	1.68	125	25	25	75
20	0.84	48	9.6	34.6	65.4
25	0.5	22	4.4	39	61
50	0.28	101	20.2	59.2	40.8
100	0.14	73	14.6	73.8	26.2
200	0.074	31	6.2	80	20

4.2.2 EDX spectroscopy

The high resolution EDX images and elemental spectra of haul road dust are described through Figure 4.1 & 4.2) of spectrum 1 corresponding to the first sample. The weight percentage of major elements like carbon, aluminum, silica, oxygen, potassium and iron as found from the spectra is graphically represented in Figures 4.3.

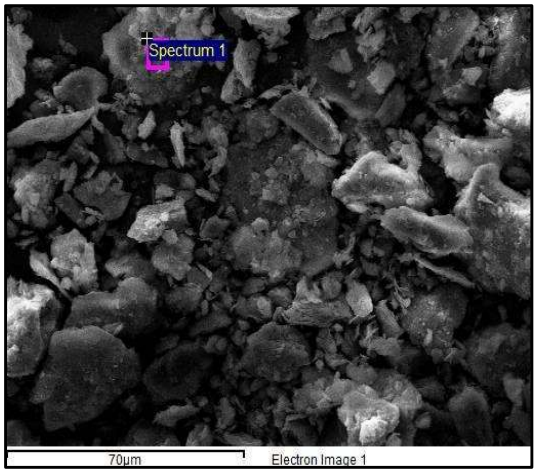

Figure 4.1 Spectrum 1: EDX image of haul road dust

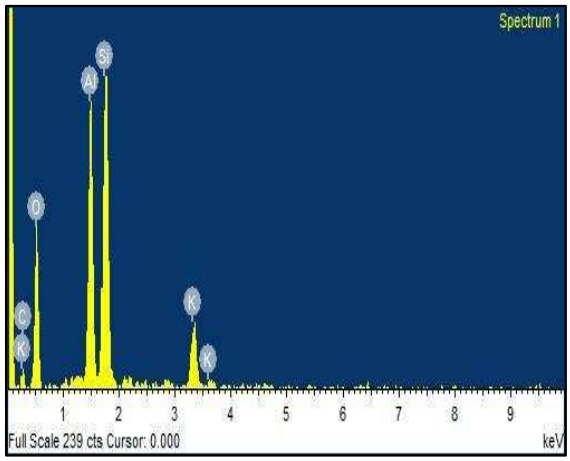

Figure 4.2 Spectrum 1: Elemental spectrum of haul road dust

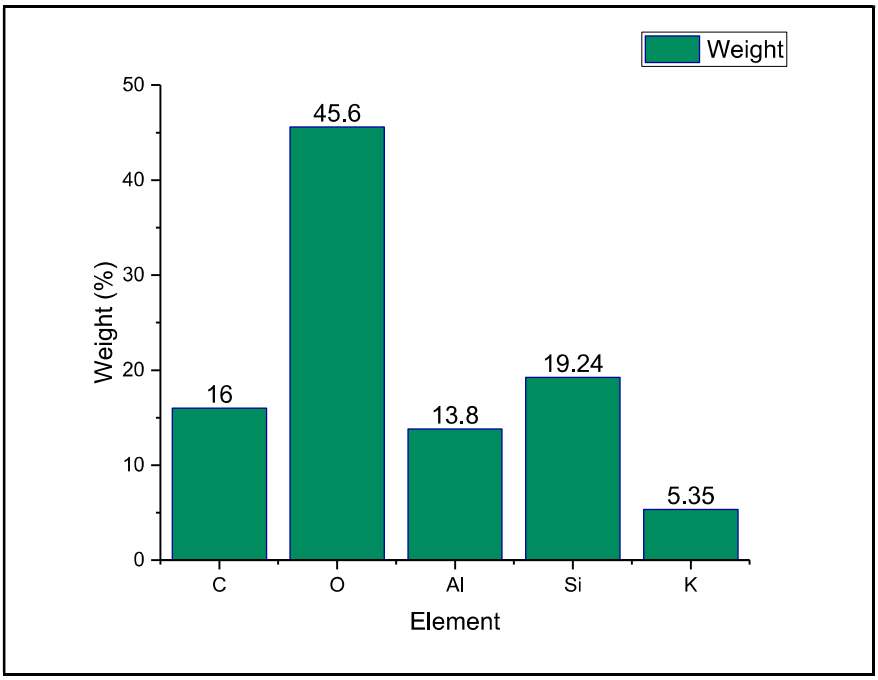

Figure 4.3 Weight % of elements present in haul road dust of spectrum 1

In the similar way, weight percentage of these elements have been obtained for three more dust samples.

Out of the study of the four dust samples the average weight percentages of the major elements have been calculated and presented in Table 4.2.

The weight % of carbon is high because of spilling over of coal pieces during transportation by haul trucks. The weight percentage of oxygen is high which indicates that oxides of silica, carbon, aluminum etc. are present in high proportion in the haul road dust.

Table 4.2 Average weight percentage of elements present in haul road

Elements	**Weight %**
Oxygen (O)	43.80
Carbon (C)	23.47
Silicon (Si)	16.68
Aluminum (Al)	11.02
Potassium (K)	4.16
Titanium (Ti)	0.55
Iron (Fe)	0.27
Other	0.05

4.3 Characterization of Synthesized Polymers

Laboratory synthesized polymers were characterized by nuclear magnetic resonance of hydrogen atom (^{1}H NMR) spectroscopy, fourier transform infrared (FTIR) spectroscopy, thermo-gravimetric analysis (TGA), intrinsic viscosity measurement, molecular weight, and neutralization equivalent measurement.

Important of different tests

- ^{1}H NMR spectroscopy and FTIR spectroscopy: Identifying whether polymerization, hydrolysis, grafting and co-polymerization have taken place or not.
- TGA: To know the thermal stability of polymer.
- Viscosity: To estimate the molecular weight of the synthesized polymers.
- Neutralization equivalent: To know the amount of partial hydrolysis.

4.4 ^{1}H NMR Spectroscopy

4.4.1 Polyacrylamide (PAM)

PAM is characterized by ^{1}H NMR spectroscopic study and the respective spectra are shown in Figure 4.4. A broad peak observed at 2.07 ppm is attributed to the methine (−CH) protons present in acrylamide units. The peak observed at 1.51 ppm is because of the methylene ($-CH_2$) protons present in polyacrylamide. The spectrum at 4.72 ppm belongs to hydrogens of deuterium oxide (HOD), which is used as solvent. The characteristic signals of N−H protons of amide groups present in polyacrylamide units are exchanged by hydrogen present

in deuterium oxide and thus no corresponding peak is observed. Therefore, the ^{1}H NMR spectroscopic data confirms the formation of polyacrylamide polymer.

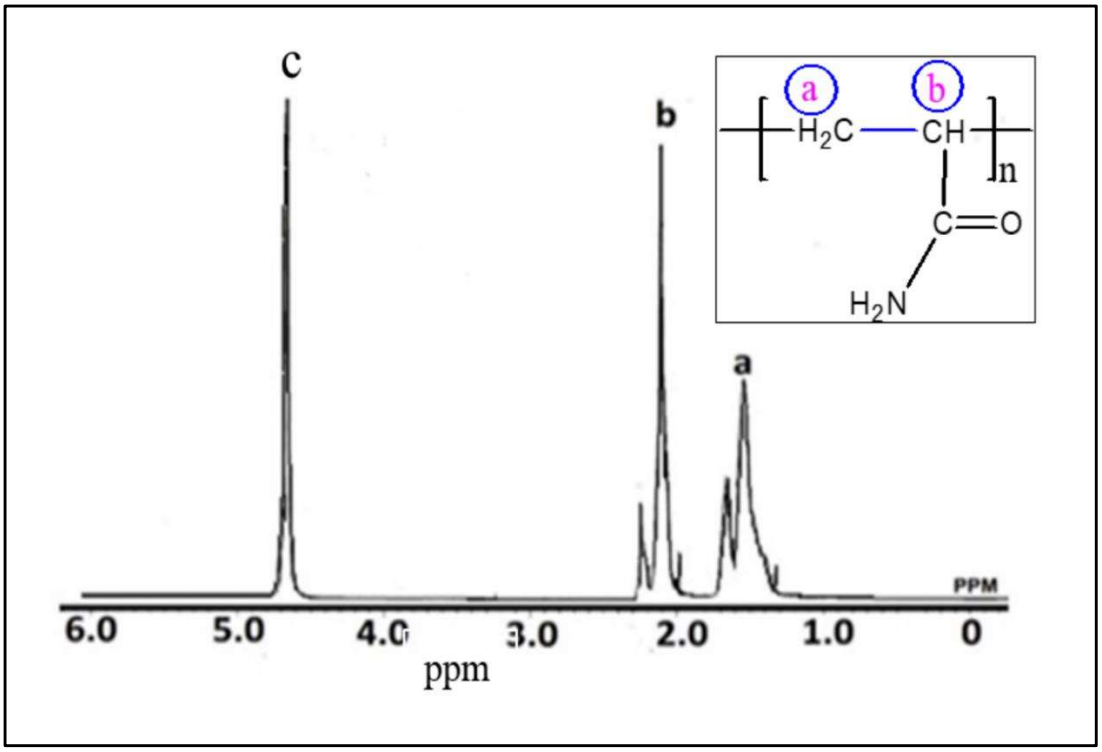

Figure 4.4 ^{1}H NMR spectra of PAM

4.4.2 Hydrolyzed Polyacrylamide (H-PAM)

H-PAM is characterized by ^{1}H NMR spectroscopic study and its respective spectra are shown in Figure 4.5. ^{1}H NMR spectra of H-PAM is almost similar to ^{1}H NMR spectra of PAM, because only amide group is converted into carboxylate group through hydrolysis. In H-PAM, only the peak at 4.67 ppm is broader than PAM peak at the same position.

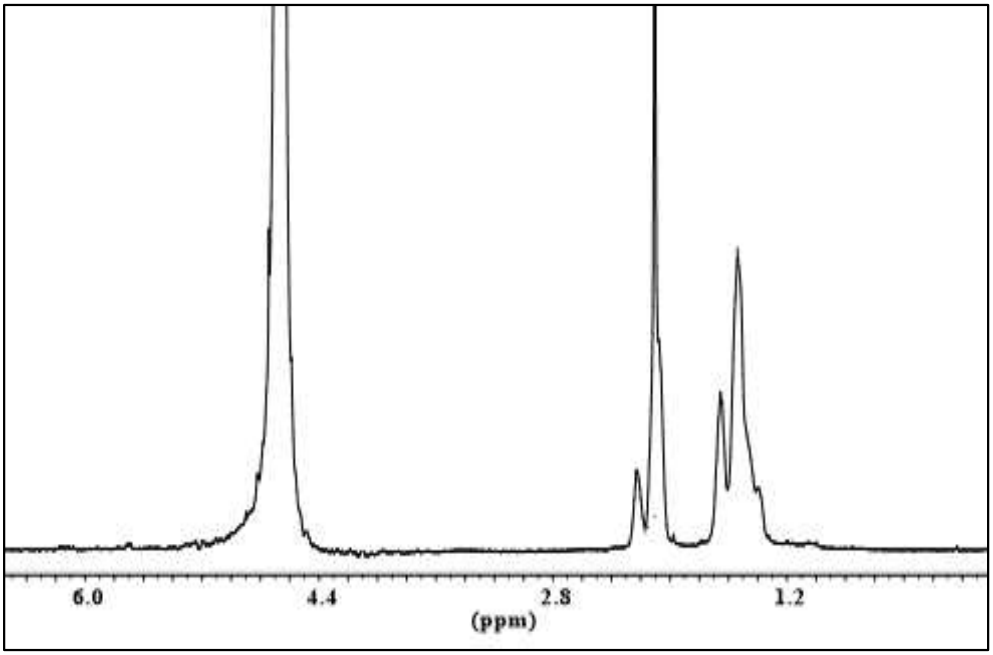

Figure 4.5 ^{1}H NMR spectra of H-PAM

4.4.3 Amylopectin-grafted- Polyacrylamide (AP-g-PAM)

The grafting of PAM over AP is confirmed by NMR spectroscopy (Figure 4.6). The resonance band of 4.5 to 4.9 ppm is attributed to the proton of deuterium oxide (HOD). The peaks at 1.3 to 1.6 ppm and 1.9 to 2.1 ppm are recognized to be the hydrogens of CH_2 and CH groups of PAM respectively. The peaks at 3.4 ppm and 3.65 ppm are hydrogens attached to carbons in anomeric and primary CH_2O- group of amylopectin respectively. These results prove that PAM was grafted over amylopectin.

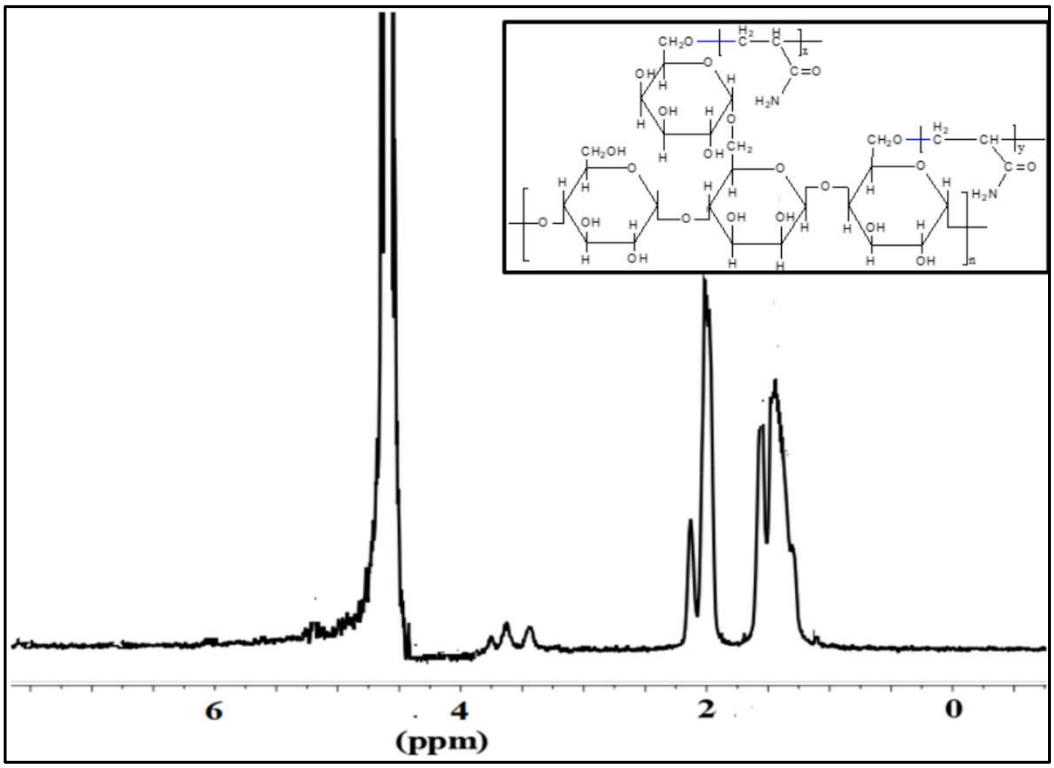

Figure 4.6 ^{1}H NMR spectra of AP-g-PAM

4.4.4 Hydrolyzed -Amylopectin-grafted- Polyacrylamide (H-AP-g-PAM)

^{1}H NMR spectra of H-AP-PAM is more or less similar to ^{1}H NMR spectra of AP-PAM. The amide group is converted into carboxylate group through hydrolysis. In H-AP-g-PAM, only the peak between 4.5 to 4.9 ppm is broader than AP-g-PAM peak at same position.

4.4.5 Guargum-grafted- Polyacrylamide (GG-g-PAM)

In Figure 4.7, the peaks at 1.5 ppm and 2.1 ppm are the protons of CH_2 and CH groups of polyacrylamide chain respectively. The peak at 3.2 ppm is the hydrogens of carbon in anomeric group of guar gum. The peak at 3.7 ppm is due to hydrogens attached to carbons in CH_2O groups of guar gum. The peak of 4.5 to 4.75 ppm is attributed to the protons of

HOD. These peaks prove that PAM and guar gum both are present in synthesized grafted polymer.

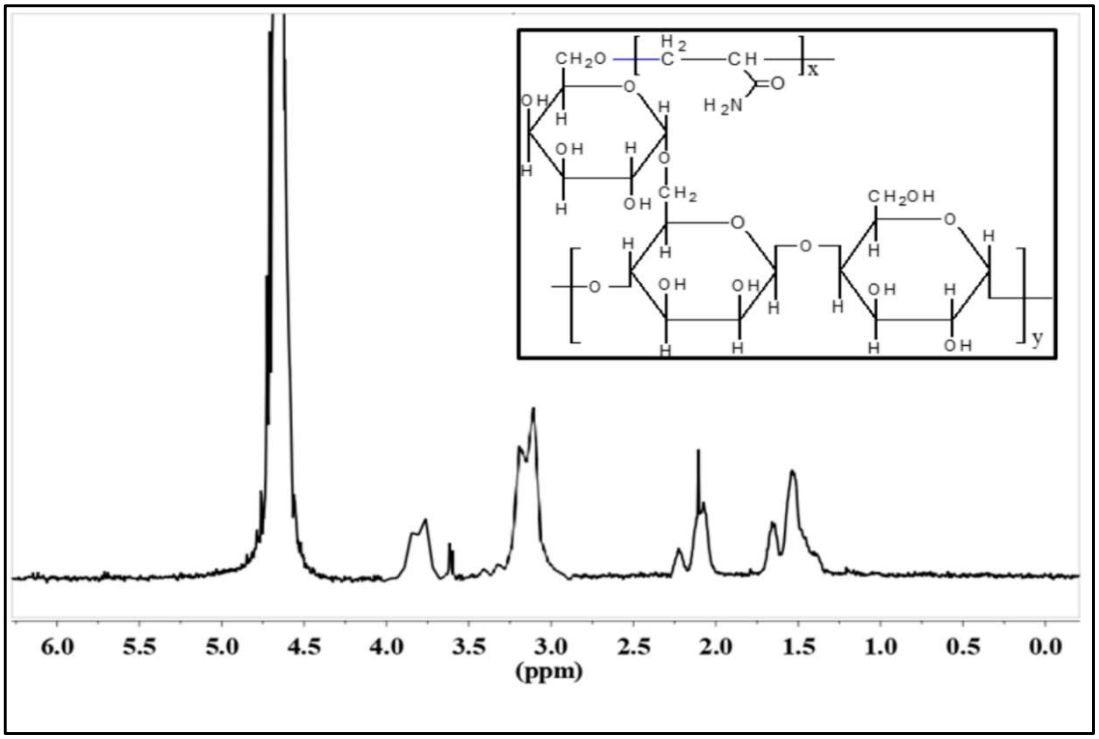

Figure 4.7 ^{1}H NMR spectra of GG-g-PAM

4.4.6 Hydrolyzed-Guargum-grafted-Polyacrylamide (H-GG-g-PAM)

^{1}H NMR spectra of H-GG-g-PAM is nearly same as ^{1}H NMR spectra of GG-g-PAM. In H-GG-g-PAM, the amide group is converted into carboxylate group through hydrolysis. The peak between 4.5 to 4.75 ppm is broader than GG-g-PAM peak at same position.

4.4.7 Poly (2-acrylamido-2-methyl-1-propanesulfonic) acid-co-Polyacrylamide (PAMPS-co-PAM)

PAM-co-PAMPS is characterized by ^{1}H NMR spectroscopic study and their respective spectra are shown in Figure 4.8. The spectrum at 4.6 ppm belongs to hydrogens of HOD, which is used as solvent. Deuterium is exchanged with protons of NH_2. The peaks at 1.3 to 1.6 ppm are attributed to the hydrogens of CH_3 of PAMPS and CH_2 of PAM & PAMPS. The peak at 2.1 ppm belongs to hydrogen present in –CH of PAM. The peak at 3.2 is for $–CH_2$ in PAMPS. The results prove that PAM and PAMPS are present in the synthesized graft copolymer.

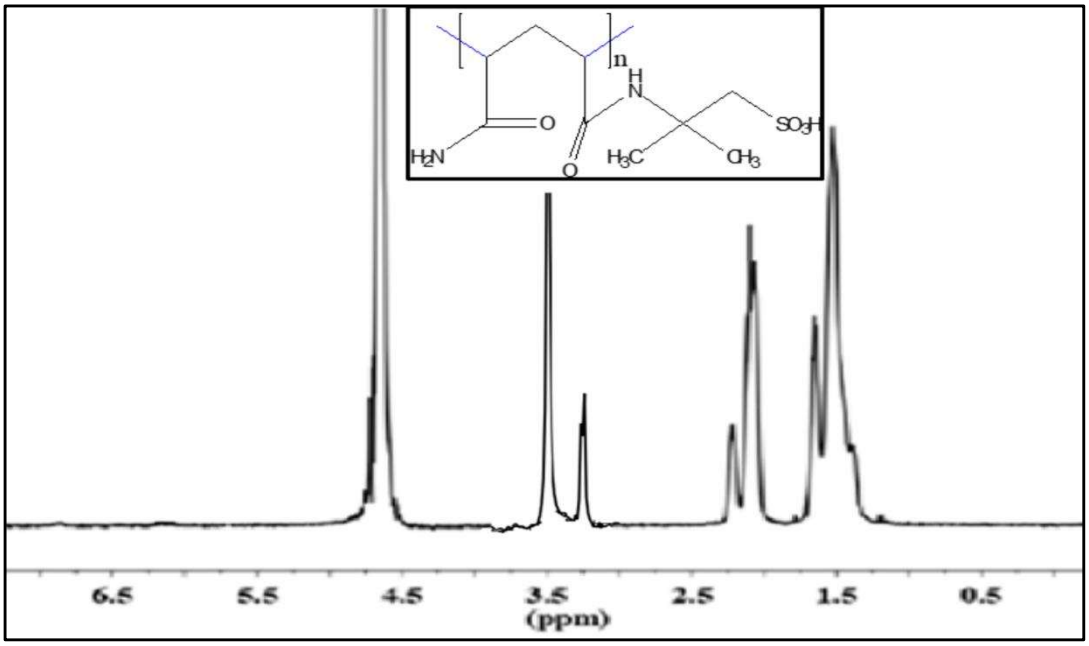

Figure 4.8 ^{1}H NMR spectra of PAMPS-co-PAM

4.4.8 Hydrolyzed Poly (2-acrylamido-2-methyl-1-propanesulfonic) acid - co-Polyacrylamide (H-PAMPS-co-PAM)

^{1}H NMR spectra is nearly the same as ^{1}H NMR spectra of PAMPS-co-PAM, since the amide group converted into carboxylate group through hydrolysis. In H-PAMPS-co-PAM, peak at 4.6 ppm and 1.3 to 1.6 are broader than PAMPS-co-PAM peak at same position.

4.5 FTIR Spectroscopy

4.5.1 Polyacrylamide (PAM)

Synthesized polyacrylamide was characterized by IR spectroscopy and its spectra are shown in Figure 4.9. Broad bands at 1633 cm^{-1} and 1603 cm^{-1} are due to the stretching vibrations of the >C=O group and bending vibration of NH_2 group respectively. Absorption bands at 1464 and 1408 cm^{-1} are due to the scissor and bending vibrations of CH_2 and CH-CO groups, respectively. Furthermore, the absorption band at 2922 cm^{-1} corresponds to the stretching vibrations of CH groups. A broad absorption band at 3437 cm^{-1} is due to the absorption band of N-H group. Finally, the absorption bands at 1350 cm-^{1} region are due to the stretching vibrations of C-N group, while the broad absorption bands in the region of 600 to 700 cm^{-1} are due to out-of-plane bending vibration of NH_2 group.

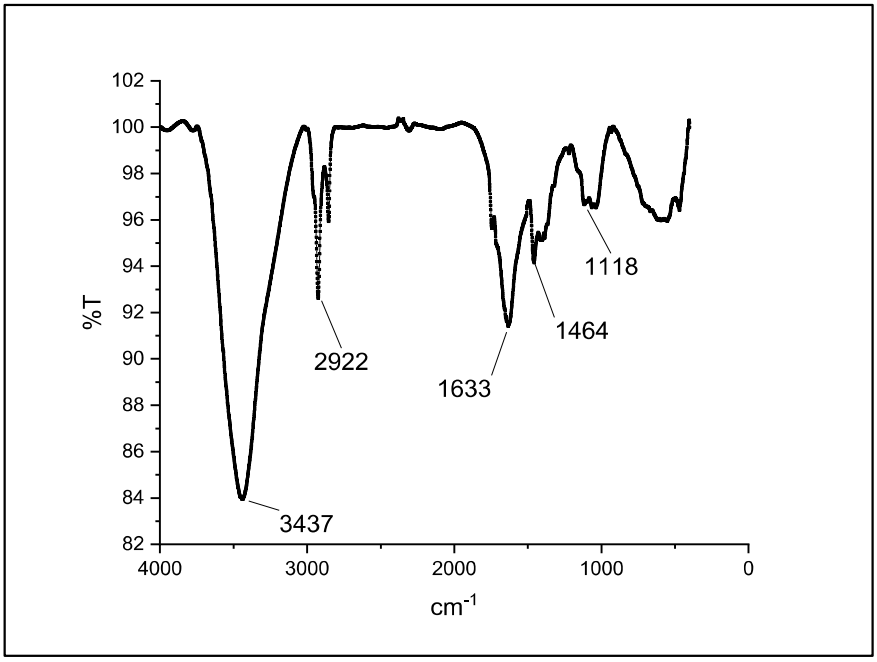

Figure 4.9 IR Spectra of PAM

4.5.2 Hydrolyzed Polyacrylamide (H-PAM)

Hydrolysis of polyacrylamide is done by NaOH. The NH_2 group is partially replaced by carboxylate group ($-COO^-Na^+$). All the peaks are similar to the PAM. The only difference between FTIR spectra of PAM and H-PAM is the adsorption band at 1341 cm^{-1} observed for C-O bond in H-PAM which is absent in PAM (Figure 4.10).

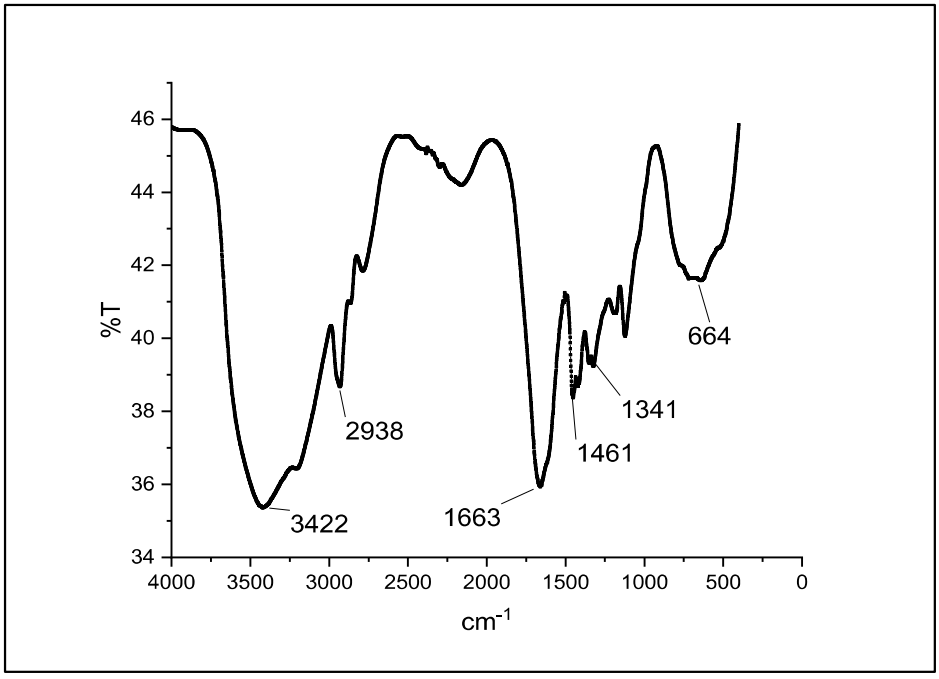

Figure 4.10 IR Spectra of H-PAM

4.5.3 Amylopectin-grafted-Polyacrylamide (AP-g-PAM)

The synthesized AP-g-PAM is characterized by FTIR spectroscopy and its spectra are shown in Figure 4.11. Absorption at 1120 cm^{-1} and between 1250 cm^{-1} to 1440 cm^{-1} is due to C-O stretching and C-O-H bending bands of amylopectin respectively. Absorption band between 2925 cm^{-1} to 2853 cm^{-1} is due to C-H stretching bands. The absorption band at 1458 cm^{-1} is due to the stretching vibrations of C-N group, and a peak at 2853 cm^{-1} is due to stretching vibrations of C-H. A strong band at 1651 cm^{-1} is due to the bending vibration of NH_2 group. A broad peak at 3428 cm^{-1} region appears due to the overlapping of stretching band of N-H of the amide group of PAM and O-H of the hydroxyl group of AP. The appearance of all the above absorption bands in the grafted copolymer is considered as a strong confirmation that grafting has taken place in the reaction.

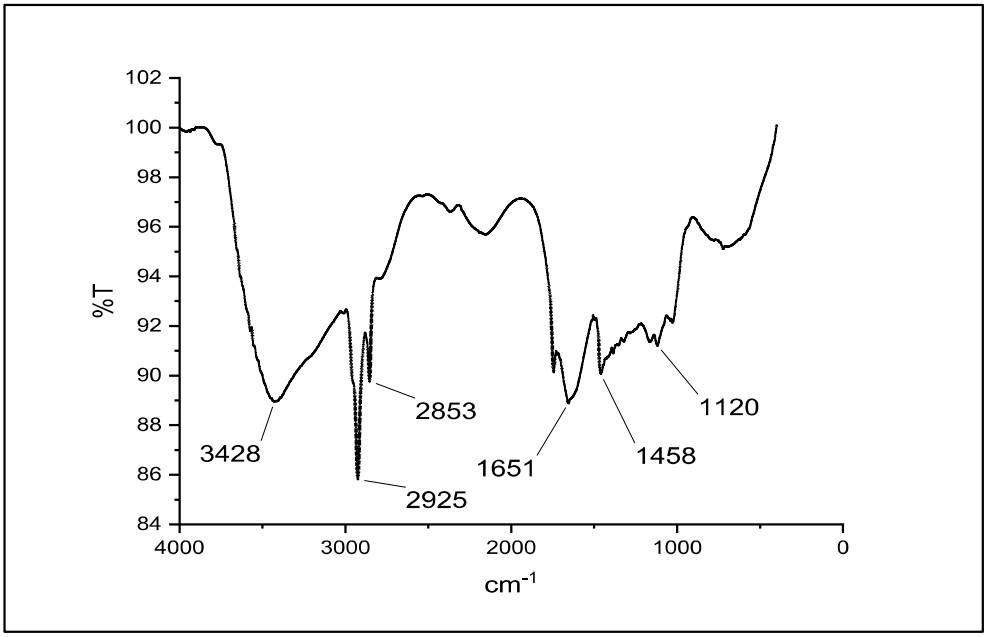

Figure 4.11 FTIR spectra of AP-g-PAM

4.5.4 Hydrolyzed-Amylopectin-grafted-Polyacrylamide (H-AP-g-PAM)

Hydrolysis of AP-g-PAM is done by NaOH. NH_2 group is partially replaced by carboxylate group (Na^+O^-). All the peaks are similar to the AP-g-PAM. Absorption peaks for –OH are also dropped between the ranges of N-H absorption bands. The only difference between FTIR peaks of AP-g-PAM and H-AP-g-PAM is the absorption band at 1216 cm^{-1} is observed for C-O bond in H-AP-g-PAM but absent in AP-g-PAM (Figure 4.12).

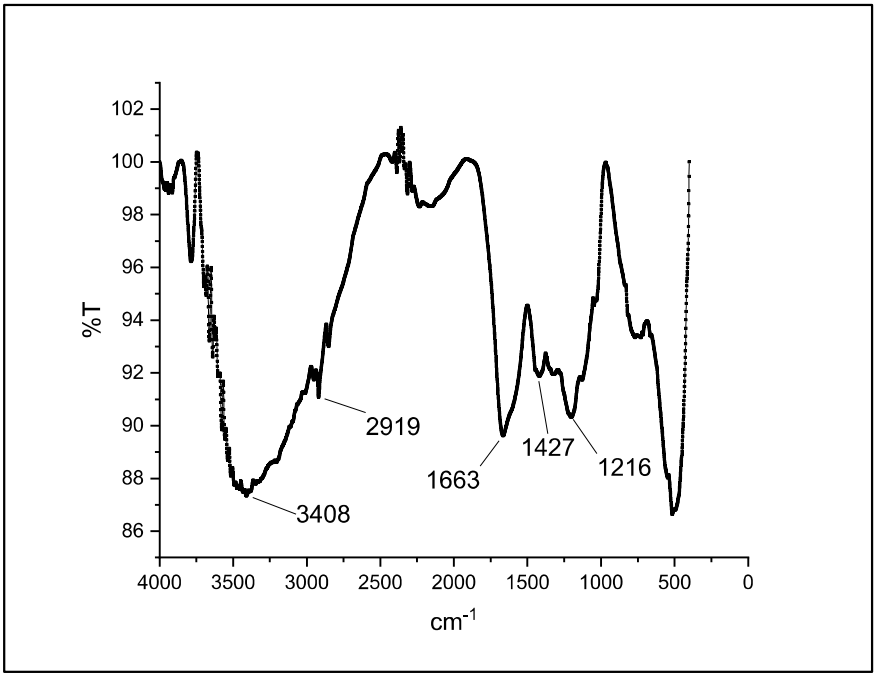

Figure 4.12 FTIR spectra of H-AP-g-PAM

4.5.5 Guargum-grafted-Polyacrylamide (GG-g-PAM)

O-H stretching band of hydroxyl group of GG and N-H stretching band of amide group of PAM overlap with each other leading to a broad band that appears at 3422 cm^{-1}. Peaks at 2926 cm^{-1} attributed to C-H stretching, 1621 cm^{-1} to C=O stretching and 1464 cm^{-1} to C-N stretching of the grafted polymer are recognized. The peak between 1430 to 1270 cm^{-1} is attributed to C-O-H bending band. C-O stretching band of GG at 1140 cm^{-1} is recognized. The peak at 692 cm^{-1} is due to out-of-plane bending vibration of NH_2. These important peaks are elucidating the structure of PAM-grafted-GG (Figure 4.13).

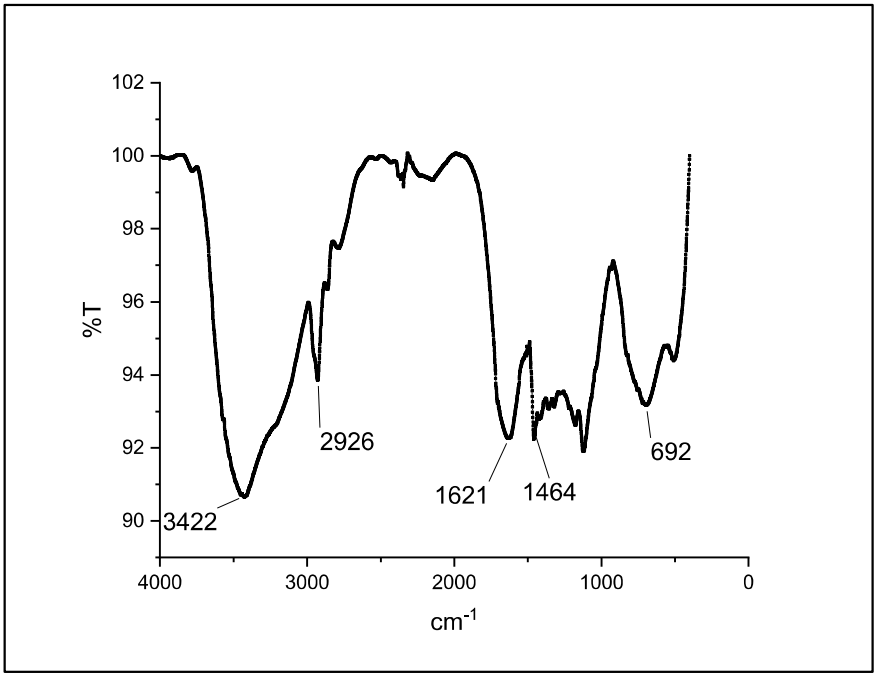

Figure 4.13 FTIR spectra of GG-g-PAM

4.5.6 Hydrolyzed-Guargum-grafted-Polyacrylamide (H-GG-g-PAM)

Hydrolysis of GG-g-PAM is done using NaOH solution. NH_2 group is partially replaced by Na^+O^- group. All the peaks are almost similar to that of GG-g-PAM (Figure 4.14). The only difference between FTIR spectra of GG-g-PAM and H-GG-g-PAM is the absorption band at 1307 cm^{-1} observed for C-O bond in H-GG-g-PAM but absent in GG-g-PAM.

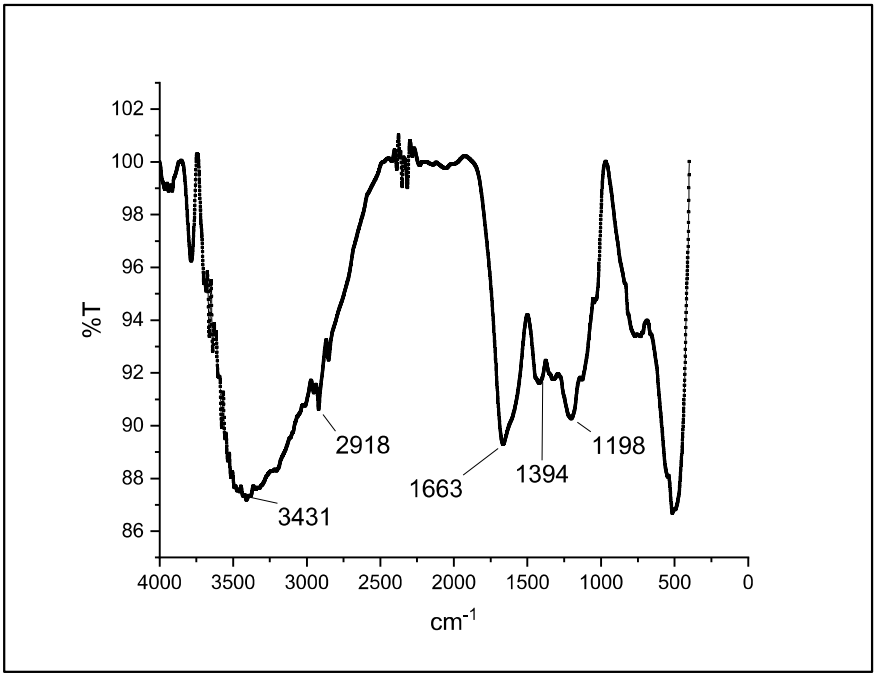

Figure 4.14 FTIR spectra of H-GG-g-PAM

4.5.7 Poly (2-acrylamido-2-methyl-1-propanesulfonic) acid-co-Polyacrylamide (PAMPS-co-PAM)

Synthesized PAMPS-co-PAM is characterized by FTIR spectroscopy, and the spectra are presented in Figure 4.15. The broad band at 3423 cm^{-1} is due to the stretching absorption band of N-H group of the PAM-co-PAMPS. At the same position (3423 cm^{-1}), stretching band of N-H of amide group and OH of hydroxyl group overlap for PAMPS. The peak at 2937 cm^{-1} is attributed to C-H stretching band. The peaks at 1675 cm^{-1} and 1451 cm^{-1} are attributed to C=O and C-N stretching bands of the co-polymer respectively. The absorption band at 1318 cm^{-1} is due to presence of SO_3^- bending vibrations in PAMPS-co-PAM. The strong stretching absorption in the region of 1039 cm^{-1} represents for S–O–C group. The appearance of all the bands are supportive proof of PAMPS-co-PAM grafting.

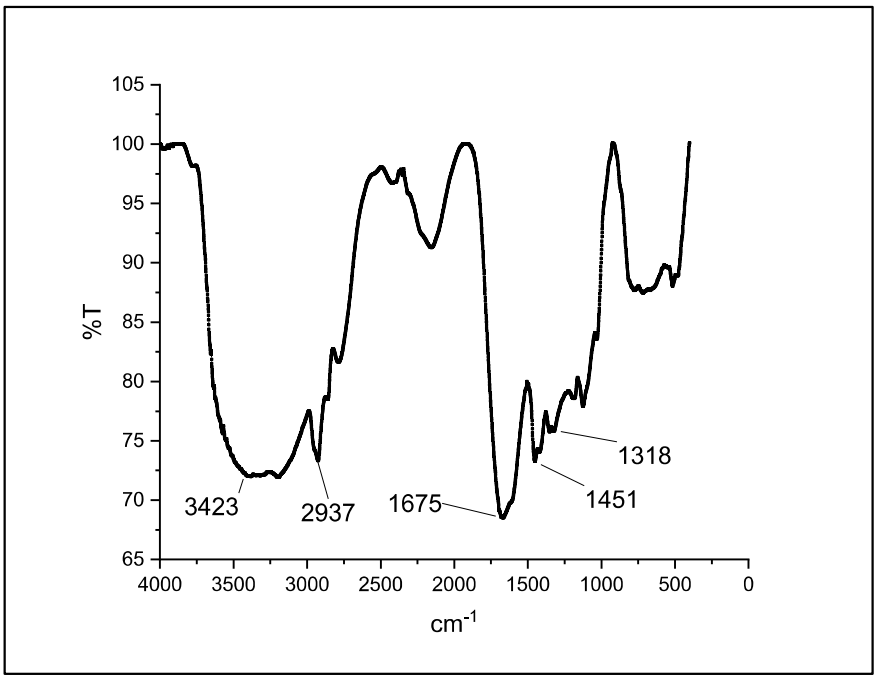

Figure 4.15 FTIR spectra of PAMPS-co-PAM

4.5.8 Hydrolyzed Poly (2-acrylamido-2-methyl-1-propanesulfonic) acid - co-Polyacrylamide (H-PAMPS-co-PAM)

Hydrolysis of PAMPS-co-PAM is done using NaOH. NH_2 group is partially replaced by Na^+O^- group. All the peaks as observed in Figure 4.16, are similar to that of PAMPS-co-PAM. –OH absorption peaks are also dropped between the ranges of N-H absorption bands. The only difference between PAMPS-co-PAM and H- PAMPS-co-PAM is the absorption band at 1282 cm^{-1} observed for C-O bond in H- PAMPS-co-PAM but absent in PAMPS-co-PAM.

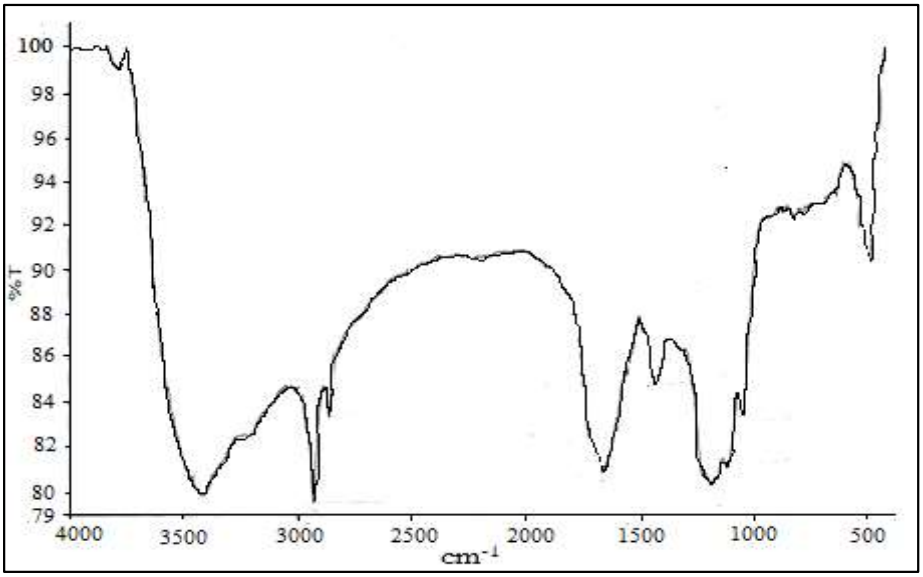

Figure 4.16 FTIR spectra of H- PAMPS-co-PAM

4.6 Thermogravimetric Analysis (TGA)

TGA curve of the synthesized polyacrylamide is shown in Figure 4.17. The mass degradation of PAM has taken place in three stages. The first weight loss of 14.34% is at 240 °C due to the evaporation of intra- and inter-molecular absorbed moisture in the PAM sample. The second degradation of 16.96% mass at 330 °C is due to loss of ammonia & carbon dioxide from the side chains of PAM. Finally, the third stage degradation of 46.7% mass is observed up to 500 °C corresponding to the degradation of PAM. From this study, it is observed that PAM has very high thermal stability at low atmospheric temperatures up to 50 °C.

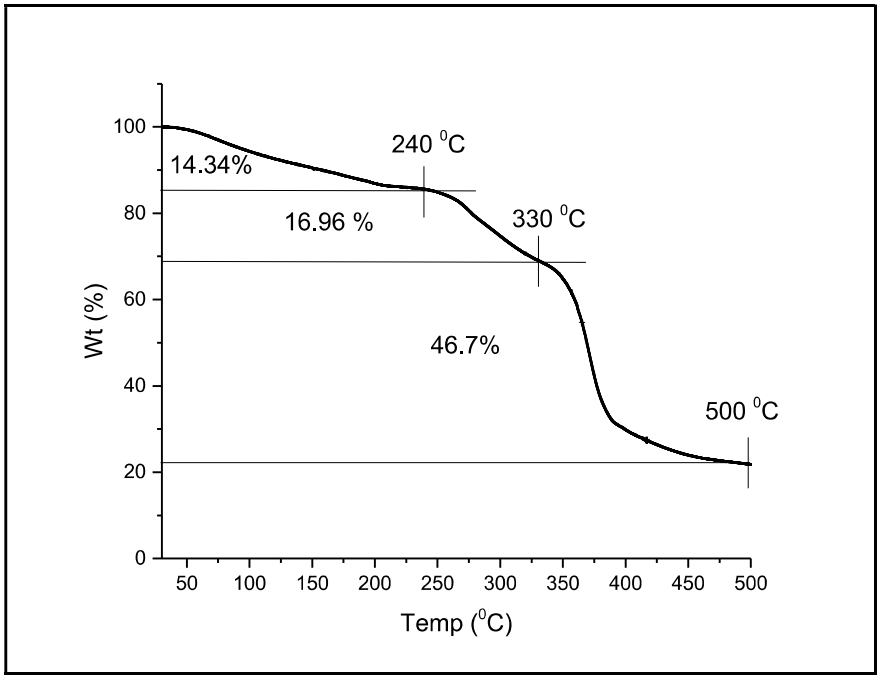

Figure 4.17 TGA curve of PAM

TGA study of the synthesized H-PAM is shown in Figure 4.18. Degradation of mass of the polymer occurs in three stages. The first weight loss of 16.42% at 200 °C is due to evaporation of intra- and inter-molecular moisture absorbed in polymer. The second weight loss of 10.48% at 300 °C corresponds to the decomposing of carbon dioxide and ammonia from side chains of polymers. The third degradation of 48% up to 500 °C is due to decomposition of the polymer. From TGA study, it is concluded that H-PAM has high thermal stability, especially below 70 °C.

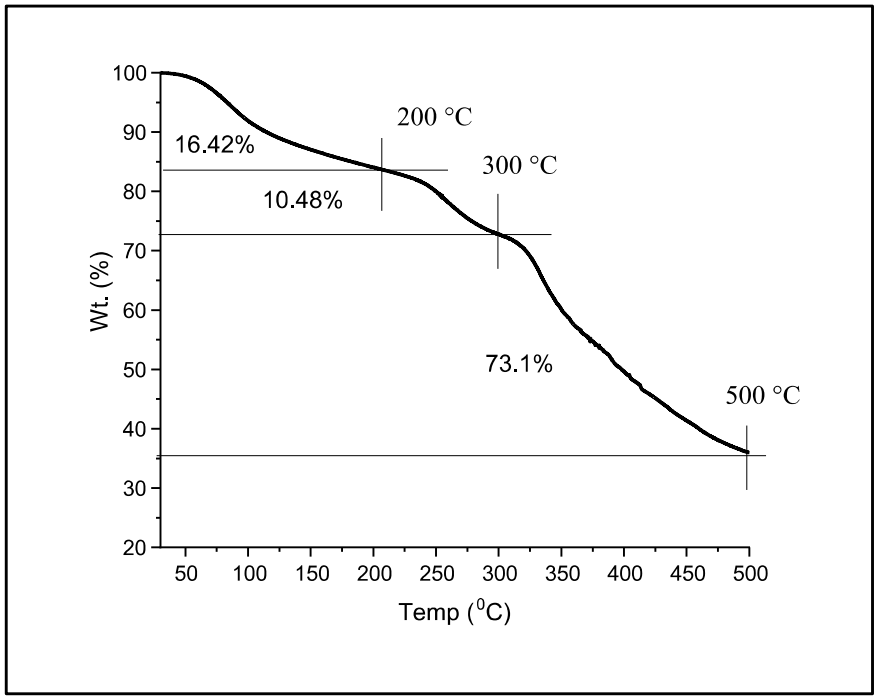

Figure 4.18 TGA curve of H-PAM

Likewise, TGA study has been carried out for AP-g-PAM, H-AP-g-PAM, GG-g-PAM, H-GG-g-PAM, PAMPS-co-PAM and H-PAMPS-co-PAM, and corresponding TGA plots are given through Figures 4.19 to 4.24.

From the TGA study it is proved that all the synthesized polymers have high thermal stability in the range of 50 °C to 70 °C.

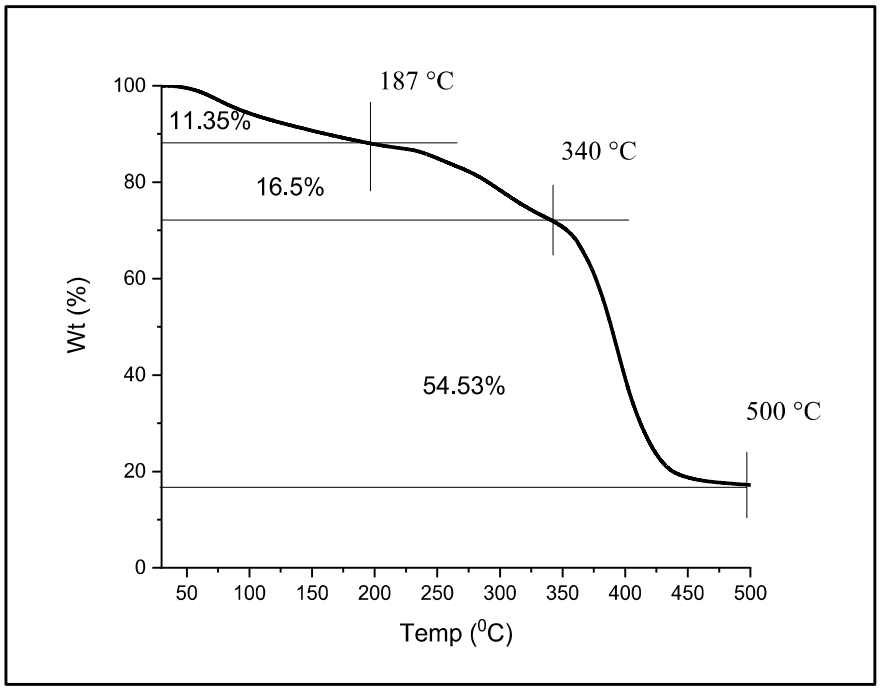

Figure 4.19 TGA curve of AP-g-PAM

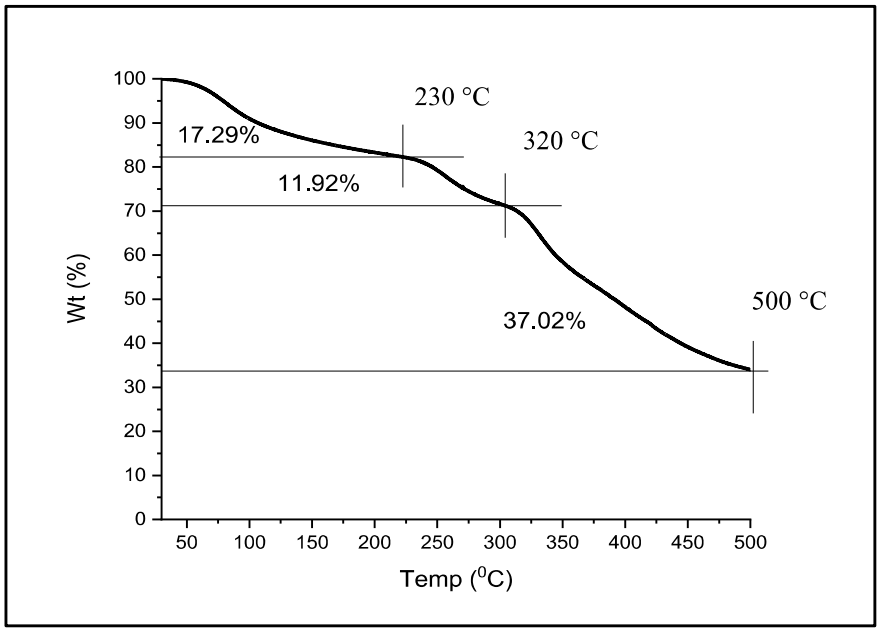

Figure 4.20 TGA curve of H-AP-g-PAM.

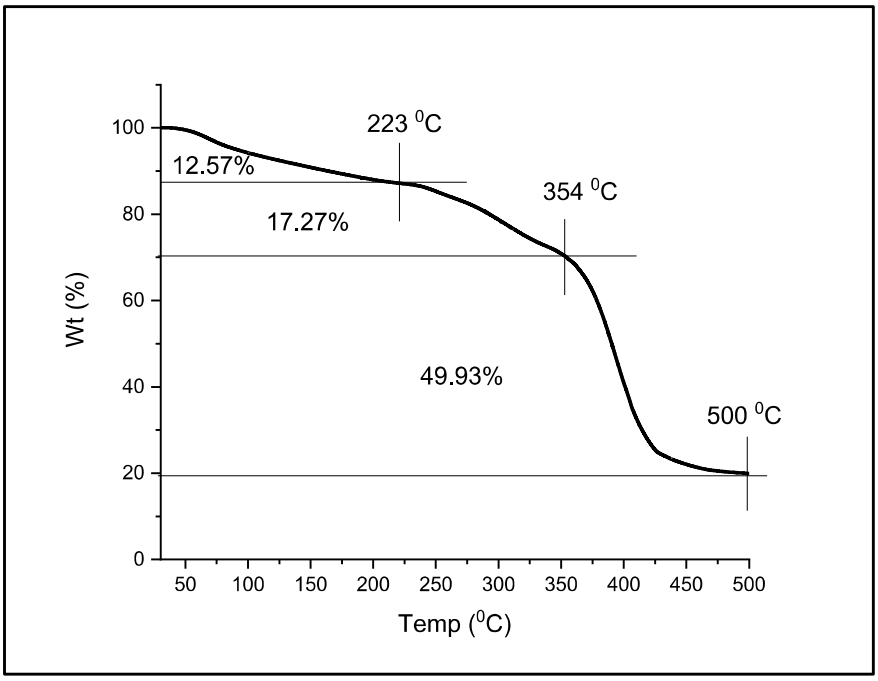

Figure 4.21 TGA curve of GG-g-PAM.

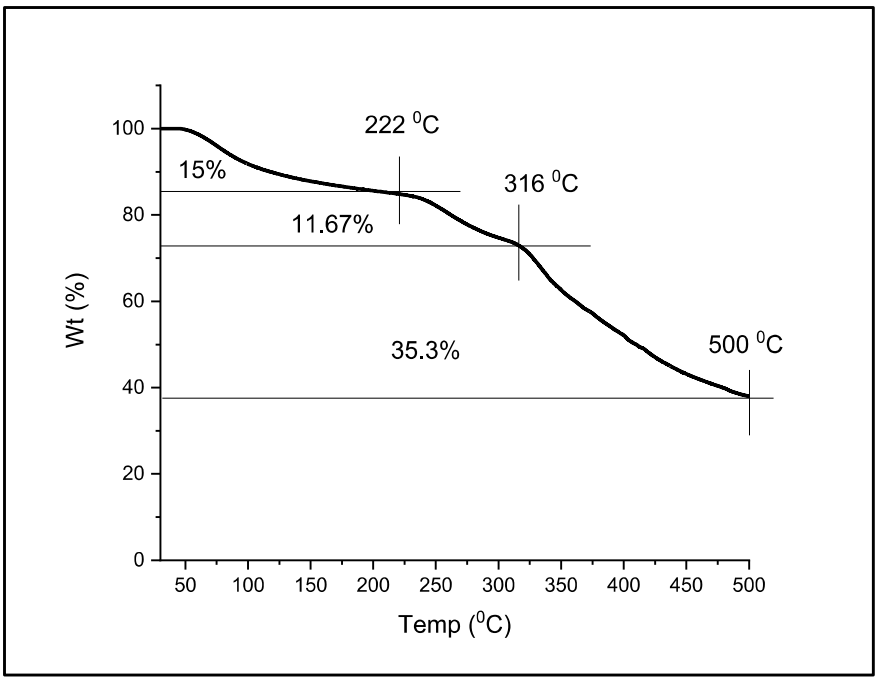

Figure 4.22 TGA curve of H-GG-g-PAM

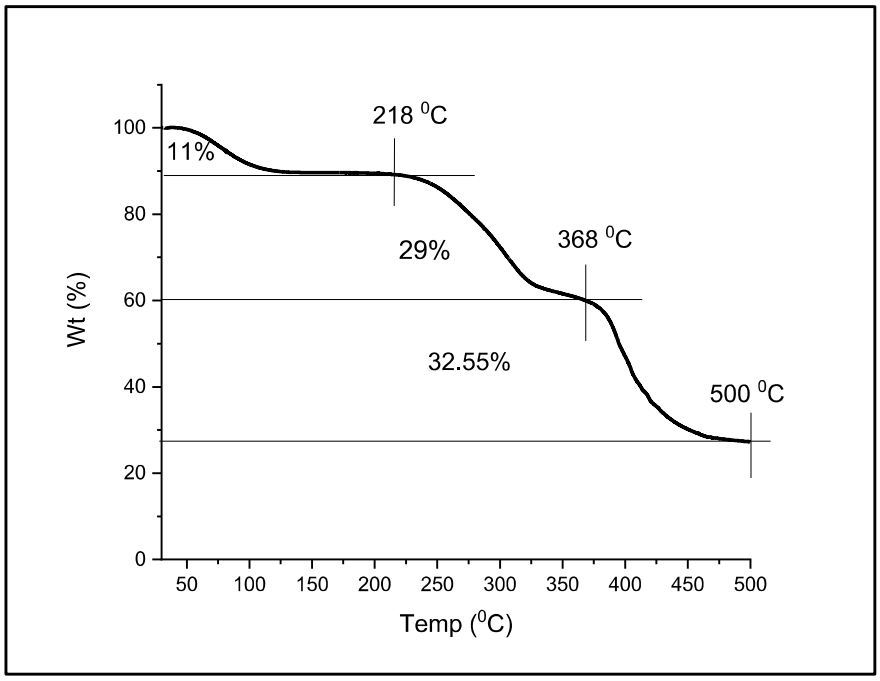

Figure 4.23 TGA curve of PAMPS-co-PAM

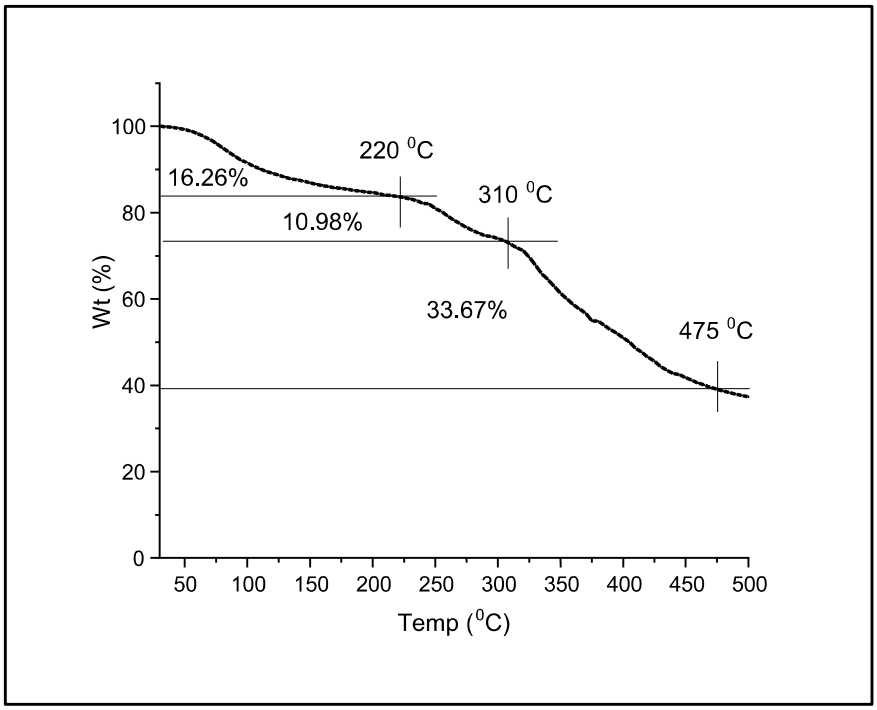

Figure 4.24 TGA curve of H- PAMPS-co-PAM

4.7 Intrinsic Viscosity Measurement

4.7.1 Polyacrylamide (PAM)

Experiment was carried out (as per the procedure discussed in section 3.7.4) with 1.0, 0.5, 0.25, 0.125 and 0.0625 g/dL concentration solutions. All calculations and their values have been shown in Table 4.3. The value of 't_0', the time of flow of distilled water is 18 s. Graphs have been plotted between reduced viscosity vs concentration, and inherent viscosity vs concentration (Figure 4.25). The intersection point of these two lines give the value of the intrinsic viscosity (η). The value of intrinsic viscosity (η) is found to be 3.33 dL/g.

Table 4.3 Calculation of reduced and inherent viscosity of PAM

S. No.	**Concent-ration, C (g/dL)**	**Flow time, t (s)**	**Reletive Viscosity, $\eta_r = t/t_0$**	**Specific Viscosity, $\eta_{sp} = \eta_r - 1$**	**Reduced viscosity, $\eta_{red} = (\eta_{sp}/C)$ (dL/g)**	**Inherent viscosity, $\eta_{red} = (\ln \eta_r)/C$ (dL/g)**
1	1	271	15.06	14.06	14.06	2.71
2	0.5	87.2	4.84	3.84	7.69	3.16
3	0.25	44.5	2.47	1.47	5.89	3.62
4	0.125	27.3	1.52	0.52	4.13	3.33
5	0.0625	22.2	1.23	0.23	3.73	3.36

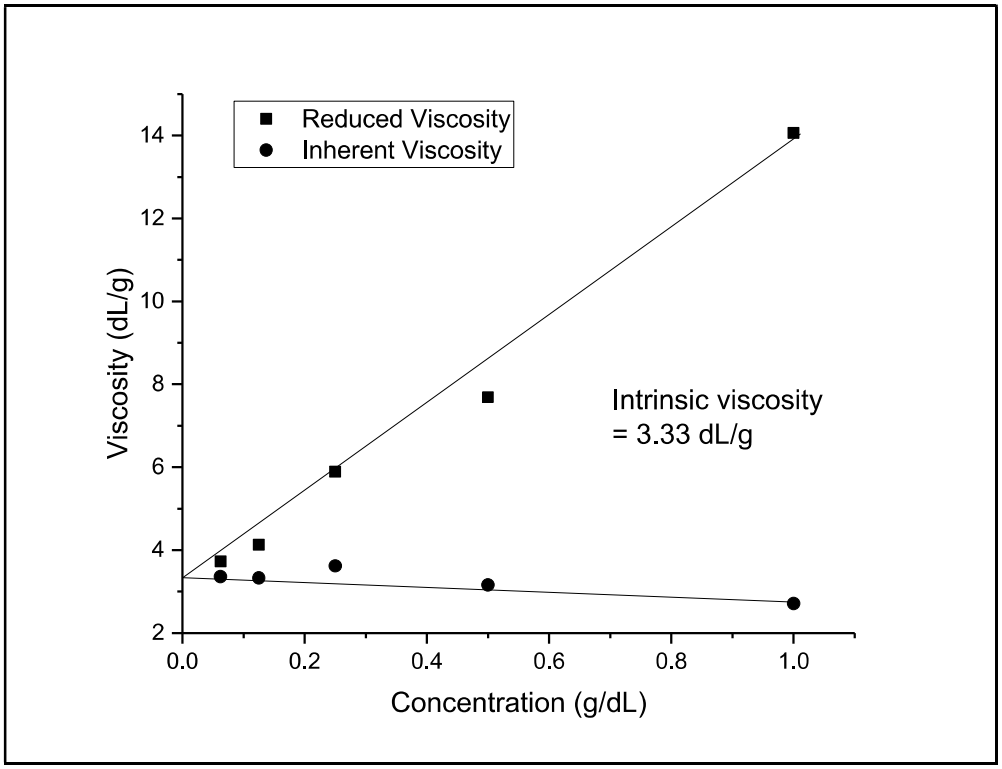

Figure 4.25 Intrinsic viscosity plot of PAM

4.7.2 Hydrolyzed Polyacrylamide (H-PAM)

All calculations and their values have been shown in Table 4.4. A graph has been plotted between reduced viscosity vs concentration and inherent viscosity vs concentration (Figure 4.26). The value of intrinsic viscosity (η) is 9.43 dL/g.

The intrinsic viscosity of H-PAM is higher than PAM. Due to hydrolyzation of PAM, more PAM molecules dissolve in water which enhances its viscosity.

Table 4.4 Calculation of reduced and inherent viscosity of H-PAM

S. No.	Concent-ration, C (g/dL)	Flow time, t (s)	Reletive Viscosity, $\eta_r = t/t_0$	Specific Viscosity, $\eta_{sp} = \eta_r - 1$	Reduced viscosity, $\eta_{red} = (\eta_{sp}/C)$ (dL/g)	Inherent viscosity, $\eta_{red} = (\ln \eta_r)/C$ (dL/g)
1	0.50	202	11.22	10.22	20.44	4.84
2	0.25	98	5.44	4.44	17.78	6.78
3	0.125	49	2.72	1.72	13.78	8.01
4	0.0625	31	1.72	0.72	11.56	8.70
5	0.0313	24	1.33	0.33	10.67	9.21

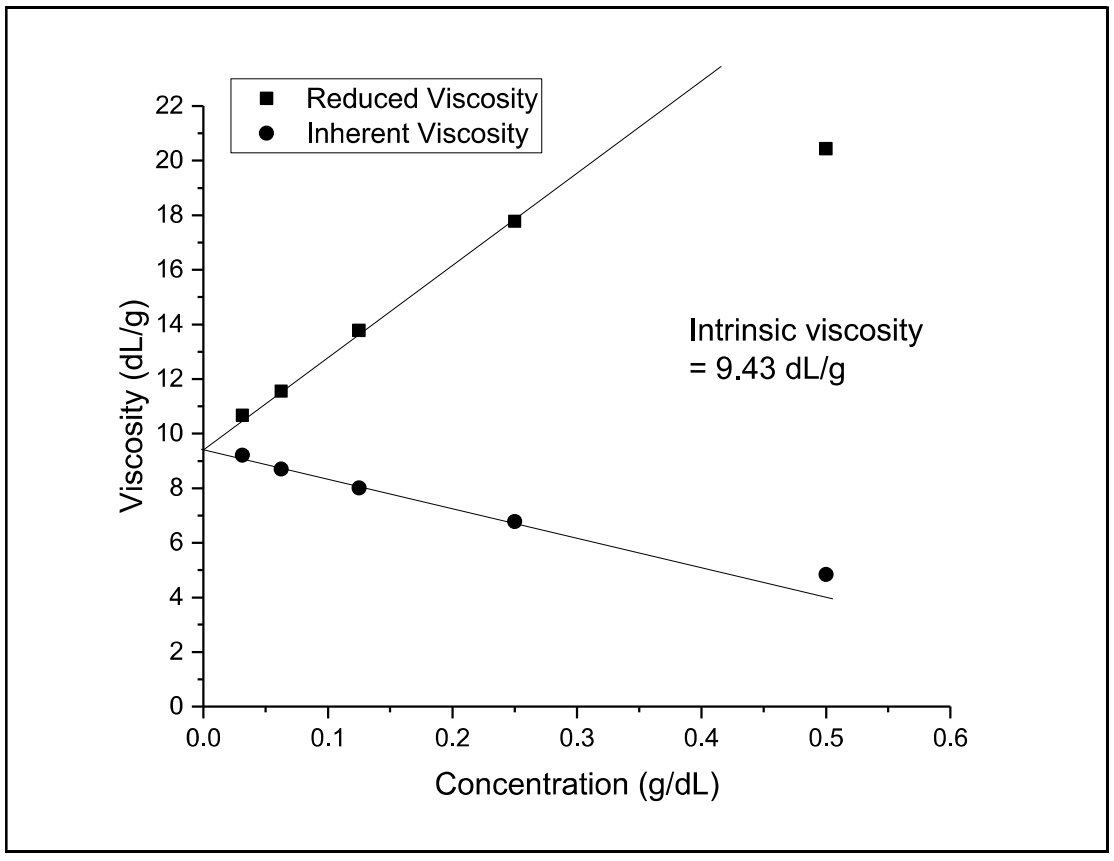

Figure 4.26 Intrinsic viscosity plot of H-PAM

In the same manner, intrinsic viscosity study has been done for AP-g-PAM, H-AP-g-PAM, GG-g-PAM, H-GG-g-PAM, PAMPS-co-PAM and H-PAMPS-co-PAM, and their corresponding plots are given through Figures 4.27 to Figures 4.32.

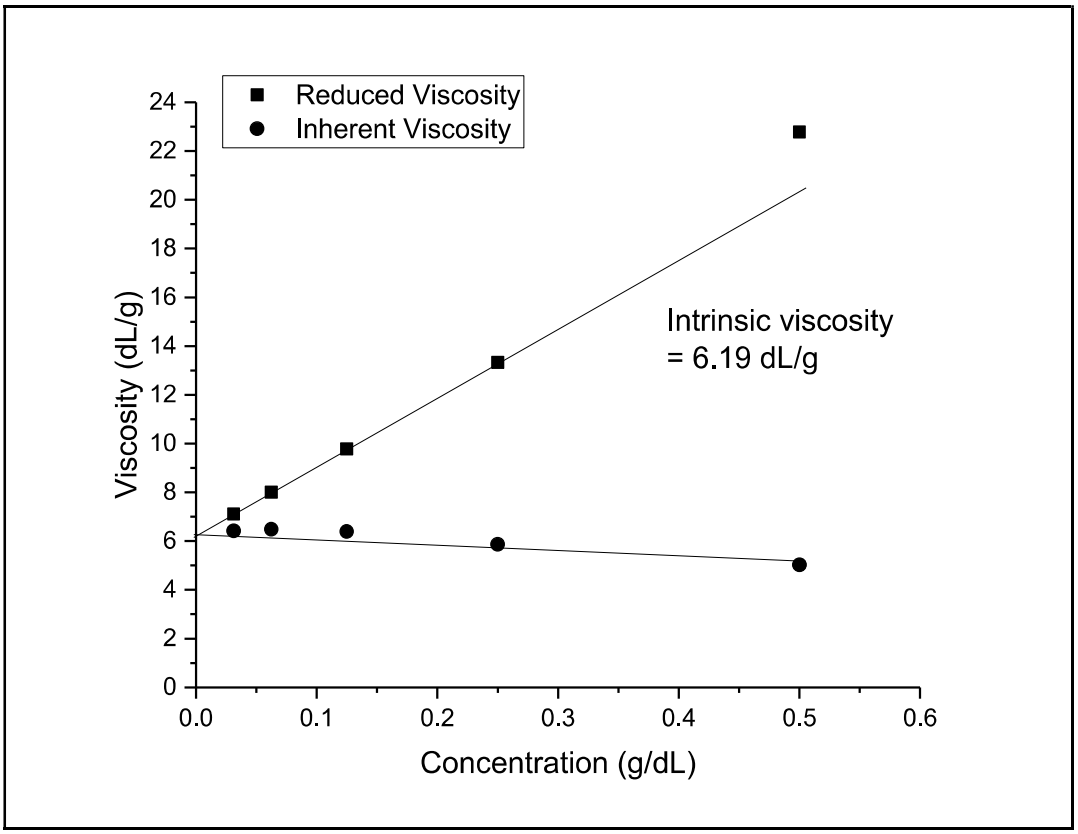

Figure 4.27 Intrinsic viscosity plot of AP-g-PAM

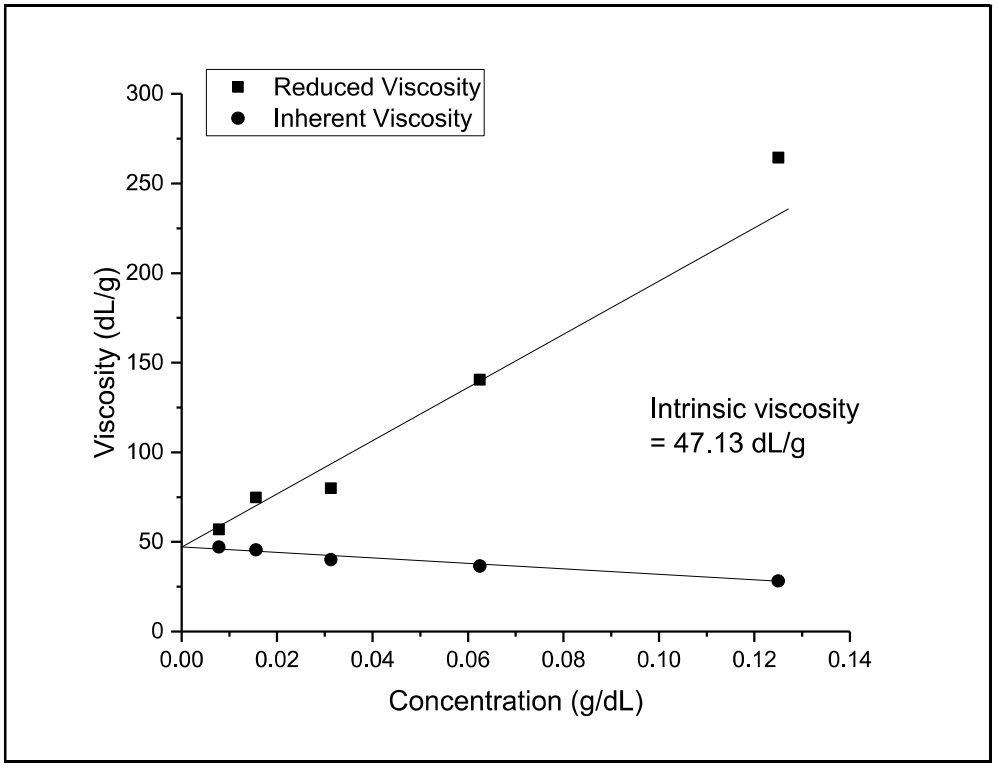

Figure 4.28 Intrinsic viscosity plot of H-AP-g-PAM

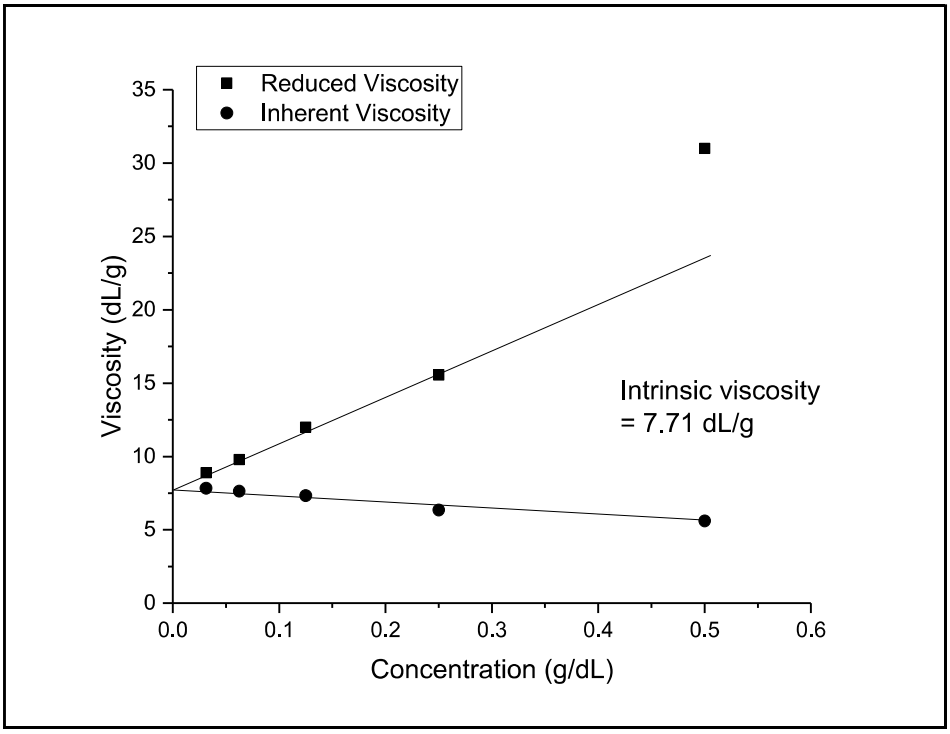

Figure 4.29 Intrinsic viscosity plot of GG-PAM

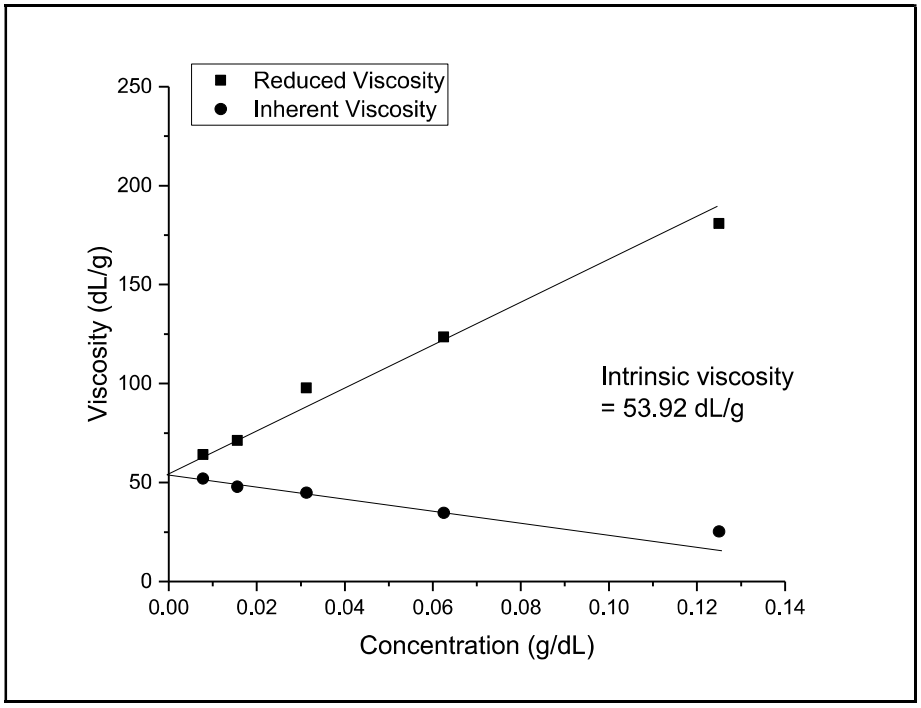

Figure 4.30 Intrinsic viscosity plot of H-GG-g-PAM

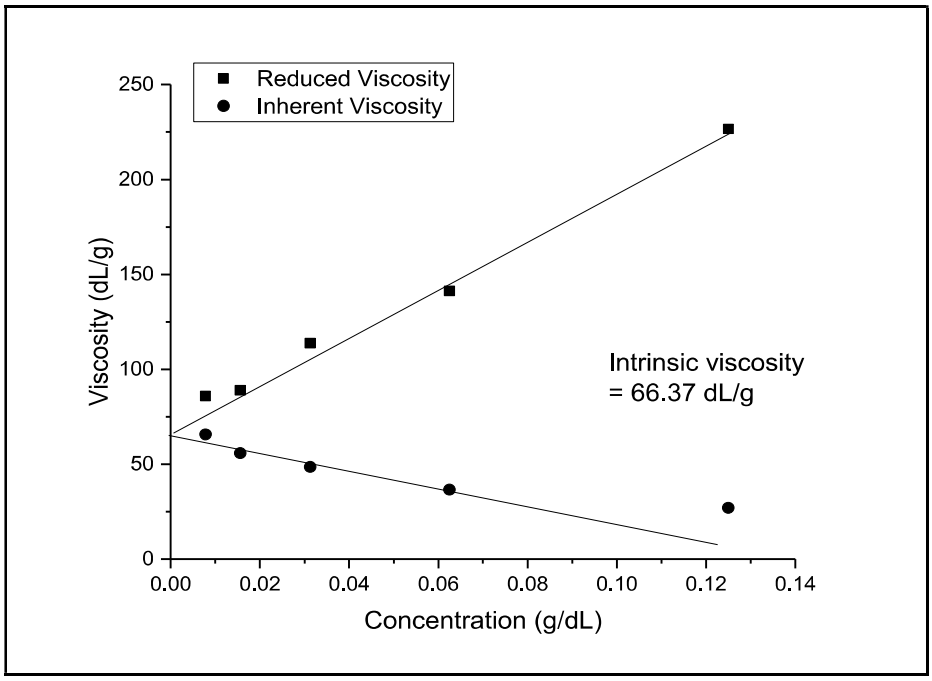

Figure 4.31 Intrinsic viscosity plot of PAM-co-PAMPS

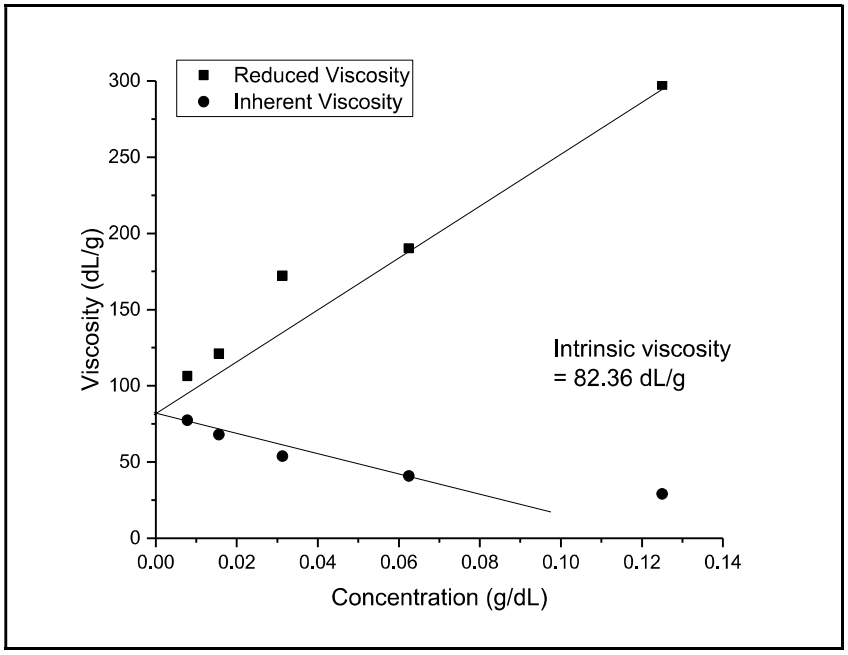

Figure 4.32 Intrinsic viscosity plot of H-PAMPS-co-PAM

Intrinsic viscosity values of all the polymers are presented in Table 4.5.

Table 4.5 Intrinsic viscosity of all polymers

Sl No.	**Polymers**	**Intrinsic viscosity (dl/g)**
1	PAM	3.33
2	Hyd-PAM	9.43
3	AP-g-PAM	6.19
4	Hyd-AP-g-PAM	47.13
5	GG-g-PAM	7.71
6	Hyd-GG-g-PAM	53.92
7	PAMPS-co-PAM	66.37
8	Hyd-PAMPS-co-PAM	82.36

4.8 Molecular Weight Measurement

The weight average molecular weight of the synthesized unhydrolyzed polymers are determined by using the Mark-Houwink equation, $[\eta] = KM^{\alpha}$ (explained in section 3.7.5). Using the values of intrinsic viscosity as shown in Table 4.5, molecular weight of the polymers are determined (Table 4.6). Molecular weight of AP-g-PAM is higher than that of PAM, which indicates that grafting has taken place in the polymerization process. Same conclusions can be drawn for the other grafted and co-polymer compounds.

Table 4.6 Molecular weight of unhydrolyzed polymers

S. No.	Polymer	Intrinsic Viscosity (dL/g) [η]	$M_w \times 10^5$ Da
1	PAM	3.33	7.99
2	AP-g-PAM	6.19	17.36
3	GG-g-PAM	7.71	22.84
4	PAMPS-co-PAM	66.37	336.84

4.9 Neutralization Equivalent Measurement

Result obtained by titration, as presented in Table 4.7 show that neutralization equivalent (NE) of H-PAM is minimum (1500) among all the hydrolyzed polymers. On the other hand, neutralization equivalent of H-PAMPS-co-PAM is the maximum (4000). For the rest two hydrolyzed polymers i.e. H-AP-g-PAM and H-GG-g-PAM, NE is 2000. As the NE increases,

solubility also increases due to more ionization. With higher solubility of polymer in water, more number of PAM molecules are available for holding the water molecules.

Table 4.7 Neutralization Equivalent of hydrolyzed polymers

Sl. No.	**Polymers**	**Neutralization Equivalent (NE)**
1	H-PAM	1500
2	H-Ap-g-PAM	2000
3	H-GG-g-PAM	2000
4	H-PAMPS-co-PAM	4000